AD-A072 926 ARMY ENGINEER WATERWAYS EXPERIMENT STATION VICKSBURG MS F/G 19/4
RESPONSE OF A MODEL ROOF SLAB TO FRAGMENT IMPACT LOADING.(U)
JUN 79 T R LUTMAN

UNCLASSIFIED WES-MP-SL-79-14 NL

1 OF 1
AD A072926

END
DATE FILMED
9-79
DDC

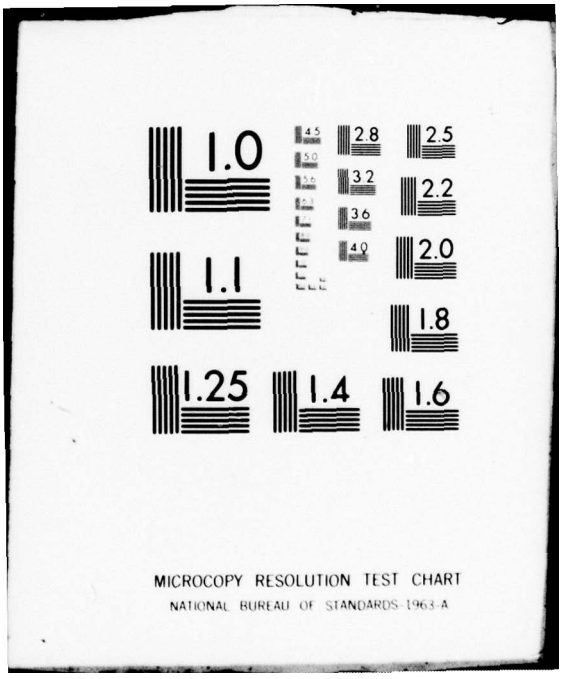
1.0
1.1
1.25
1.4
1.6
1.8
2.0
2.2
2.5
2.8
3.2
3.6
4.0
4.5
5.0
MICROCOPY RESOLUTION TEST CHART
NATIONAL BUREAU OF STANDARDS-1963-A

MISCELLANEOUS PAPER SL-79-14

RESPONSE OF A MODEL ROOF SLAB TO FRAGMENT IMPACT LOADING

by

Thomas R. Lutman
Structures Laboratory
U. S. Army Engineer Waterways Experiment Station
P. O. Box 631, Vicksburg, Miss. 39180

June 1979
Interim Report

Prepared for Office, Chief of Engineers, U. S. Army
Washington, D. C. 20314

Under Project 4A762719AT40
Task BO, Work Unit 002

Destroy this report when no longer needed. Do not return it to the originator.

The findings in this report are not to be construed as an official Department of the Army position unless so designated by other authorized documents.

Unclassified

SECURITY CLASSIFICATION OF THIS PAGE (When Data Entered)

REPORT DOCUMENTATION PAGE

READ INSTRUCTIONS BEFORE COMPLETING FORM

1. REPORT NUMBER: Miscellaneous Paper SL-79-14
2. GOVT ACCESSION NO.
3. RECIPIENT'S CATALOG NUMBER

4. TITLE (and Subtitle): RESPONSE OF A MODEL ROOF SLAB TO FRAGMENT IMPACT LOADING
5. TYPE OF REPORT & PERIOD COVERED: Interim Report
6. PERFORMING ORG. REPORT NUMBER

7. AUTHOR(s): Thomas R. Lutman
8. CONTRACT OR GRANT NUMBER(s)

9. PERFORMING ORGANIZATION NAME AND ADDRESS:
U. S. Army Engineer Waterways Experiment Station
Structures Laboratory
P. O. Box 631, Vicksburg, Miss. 39180

10. PROGRAM ELEMENT, PROJECT, TASK AREA & WORK UNIT NUMBERS: ~~Project~~ 4A762719AT40, Task B0, Work Unit 002

11. CONTROLLING OFFICE NAME AND ADDRESS:
Office, Chief of Engineers, U. S. Army
Washington, D. C. 20314

12. REPORT DATE: ~~June~~ 1979
13. NUMBER OF PAGES: 32

14. MONITORING AGENCY NAME & ADDRESS (if different from Controlling Office): WES-MP-SL-79-14

15. SECURITY CLASS. (of this report): Unclassified
15a. DECLASSIFICATION/DOWNGRADING SCHEDULE

16. DISTRIBUTION STATEMENT (of this Report)

Approved for public release; distribution unlimited.

17. DISTRIBUTION STATEMENT (of the abstract entered in Block 20, if different from Report)

37 p.

18. SUPPLEMENTARY NOTES

19. KEY WORDS (Continue on reverse side if necessary and identify by block number)

Concrete slabs	Roofs	Weapon fragmentation
Fortifications	Slabs	
Impact tests	Structural members	
Impulsive loads	Structural models	

20. ABSTRACT (Continue on reverse side if necessary and identify by block number)

Not only must structure perforation by high-speed fragment impact be considered when designing earth-covered fortifications but also the impulsive load imported by these impacts to the structure must be considered. This report describes preliminary tests and analyses conducted to determine a design procedure that will account for these loads. As an initial step, a 1/8th-scale model simply supported, one-way, reinforced-concrete roof slab 3/4 in. thick with a

(Continued)

DD FORM 1 JAN 73 1473 EDITION OF 1 NOV 65 IS OBSOLETE

Unclassified

SECURITY CLASSIFICATION OF THIS PAGE (When Data Entered)

038 100

20. ABSTRACT (Continued).

4.5-in. dense sand cover was selected for analysis and testing. Fragments having a mass of 4.41 grams were fired from a gun at velocities from 2000 to 4000 fps, impacting the center of the roof slab. Deflection-versus-time histories were monitored and compared with predictions made using an equivalent single-degree-of-freedom analysis. This analytical technique appeared to be a good means of predicting maximum response; however, more experiments are recommended before an analytical design procedure is developed.

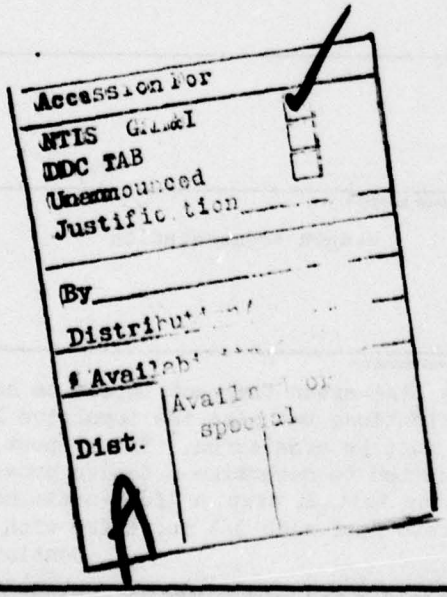

THE CONTENTS OF THIS REPORT ARE NOT TO BE USED FOR ADVERTISING, PUBLICATION, OR PROMOTIONAL PURPOSES. CITATION OF TRADE NAMES DOES NOT CONSTITUTE AN OFFICIAL ENDORSEMENT OR APPROVAL OF THE USE OF SUCH COMMERCIAL PRODUCTS.

PREFACE

This study was conducted for the Office, Chief of Engineers, U. S. Army, by personnel of the Structures Division (SD), Structures Laboratory (SL), U. S. Army Engineer Waterways Experiment Station (WES), as part of Project 4A762719AT40, Task Area B0, Work Unit 002, "Response of Structures and Engineer Materials to Artillery and Bomb Fragments."

This investigation was conducted by Cadet T. R. Lutman, class of 1979, U. S. Military Academy, during a training assignment to WES in July and August 1978. The project was directed by Mr. D. R. Coltharp, SD. Assistance with the experimental program was provided by Mr. D. F. Hale, SD.

The work was performed and report prepared under the general supervision of Messrs. B. Mather and W. J. Flathau, Chief and Assistant Chief, respectively, SL, and J. T. Ballard, Chief, SD.

COL J. L. Cannon, CE, was Director of WES during the investigation. Mr. F. R. Brown was Technical Director.

CONTENTS

CONVERSION FACTORS, U. S. CUSTOMARY TO METRIC (SI) UNITS OF MEASUREMENT

U. S. customary units of measurement used in this report can be converted to metric (SI) units as follows:

Multiply	By	To Obtain
cubic feet	0.02831685	cubic metres
cubic yards	0.7645549	cubic metres
Farenheit degrees	5/9	Celsius degrees or Kelvins*
feet	0.3048	metres
inches	2.54	centimetres
kips (force) per square inch	6894.757	kilopascals
pounds (force) per square inch	6.894757	kilopascals
pounds (mass)	0.4535924	kilograms
pounds (mass) per cubic foot	16.01846	kilograms per cubic metre

* To obtain Celsius (C) temperature readings from Fahrenheit (F) readings, use the following formula: $C = (5/9)(F - 32)$. To obtain Kelvin (K) readings, use: $K = (5/9)(F - 32) + 273.15$.

RESPONSE OF A MODEL ROOF SLAB TO FRAGMENT IMPACT LOADING

PART I: INTRODUCTION

Background

1. Recent studies at the U. S. Army Engineer Waterways Experiment Station (WES) confirmed the ability of soil coverings to protect structures from perforation by high-velocity fragments such as those produced by the detonation of artillery projectiles or bombs. These studies were also used to develop a procedure for determining the thickness of soil required to absorb the kinetic energy of the impacting fragment.

2. Previously, fortifications have been designed only to prevent the high-velocity fragments from perforating the structures. The actual effectiveness of the structure in protecting the occupants, however, is also dependent on the ability of the structural elements to withstand the load imparted through the soil covering by the fragment impact.

3. The soil absorbs the kinetic energy of the impact and then transfers that energy to the structural element. The element absorbs this energy as an impulsive load, which gives it an initial velocity. As the element proceeds through the response to this initial velocity, it deforms to some maximum deflection. If the deflection is great enough, the load imparted by the fragment can cause the structure to collapse.

4. Thus, a research effort has been initiated to investigate the structural response to fragment impact and to establish an analytical procedure for determining this response. This procedure can then be used as a criterion for designing structures that may be subjected to fragment loading. This report presents the results of preliminary research accomplished during July-August 1978.

Scope

5. The experimental program and an analysis of the fragment impact response data obtained from the test series are described briefly below. The analytical procedure for predicting the response is given and compared with the experimental results.

PART II: EXPERIMENTAL PROGRAM

Description of Test Program

6. The purpose of the program was to establish a preliminary procedure for determining response of structural elements to fragment impact and to collect data to evaluate accuracy and range of application of this procedure for design purposes. The experimental program involved normal impact of right-circular cylindrical projectiles (simulating fragments) into a model of an earth-covered concrete command and control shelter roof slab. Impact velocities ranged from 2000 to 4000 fps.*,** The data collected from each test consisted of impact velocity and a corresponding deflection-versus-time history of the response† following the fragment impact. From the deflection-versus-time history, peak deflections and the natural frequency were determined. A typical deflection-versus-time history is presented in Figure 1. A total of nine tests were conducted using steel fragments impacting on a dense-sand-covered concrete slab target.

Fragment Simulation Facility

7. The WES FSF is described fully in Reference 2. The facility consists of an underground firing range, containing the high-velocity powder gun and associated measurement systems, and an adjacent outside support building containing the firing control, electronic data acquisition systems, and equipment necessary for hand-loading cartridges (Figure 2).

---

* Reference 1 indicates that the actual range of fragment impact velocities is from 100 to about 10,000 fps. The WES Fragment Simulation Facility (FSF) system used, however, was limited to a 1000- to 4000-fps range. This range was deemed sufficient to provide elastic or low-range plastic behavior in the targets.

** A table of factors for converting U. S. customary units of measurement to metric (SI) units is presented on page 4.

† Deflection-versus-time histories were taken at the center of the roof slab element using a deflection gage.

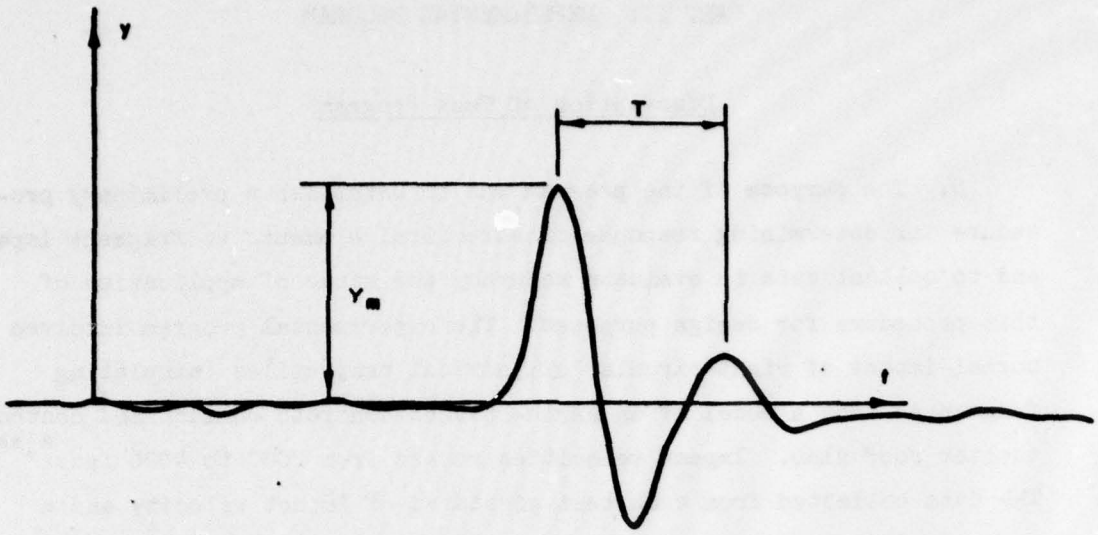

Figure 1. Typical deflection-versus-time history for center of slab

Firing Device

8. The high-velocity powder gun is described in Reference 3. However, for the purposes of this program, the low-velocity (LV) system (also discussed in Reference 3) was used. This system is shown in Figure 3 and consists of a Winchester Model 70 .458-caliber magnum bolt-action mechanism and an adapter to couple with the barrel assembly. Fragments, sabots, cartridges, and powder similar to those used in the tests described in Reference 3 were used in these tests.

Firing system and safety considerations

9. The firing system and safety considerations presented in Reference 3 are presented here for emphasis.

10. Firing was initiated by a firing control switch in the support building. The switch activated a solenoid device which was mounted on a stage, which in turn was attached below the bolt-action mechanism (Figure 3). The solenoid ram impacted the trigger with sufficient force to fire the round.

11. Safety considerations in the firing sequence were simple and

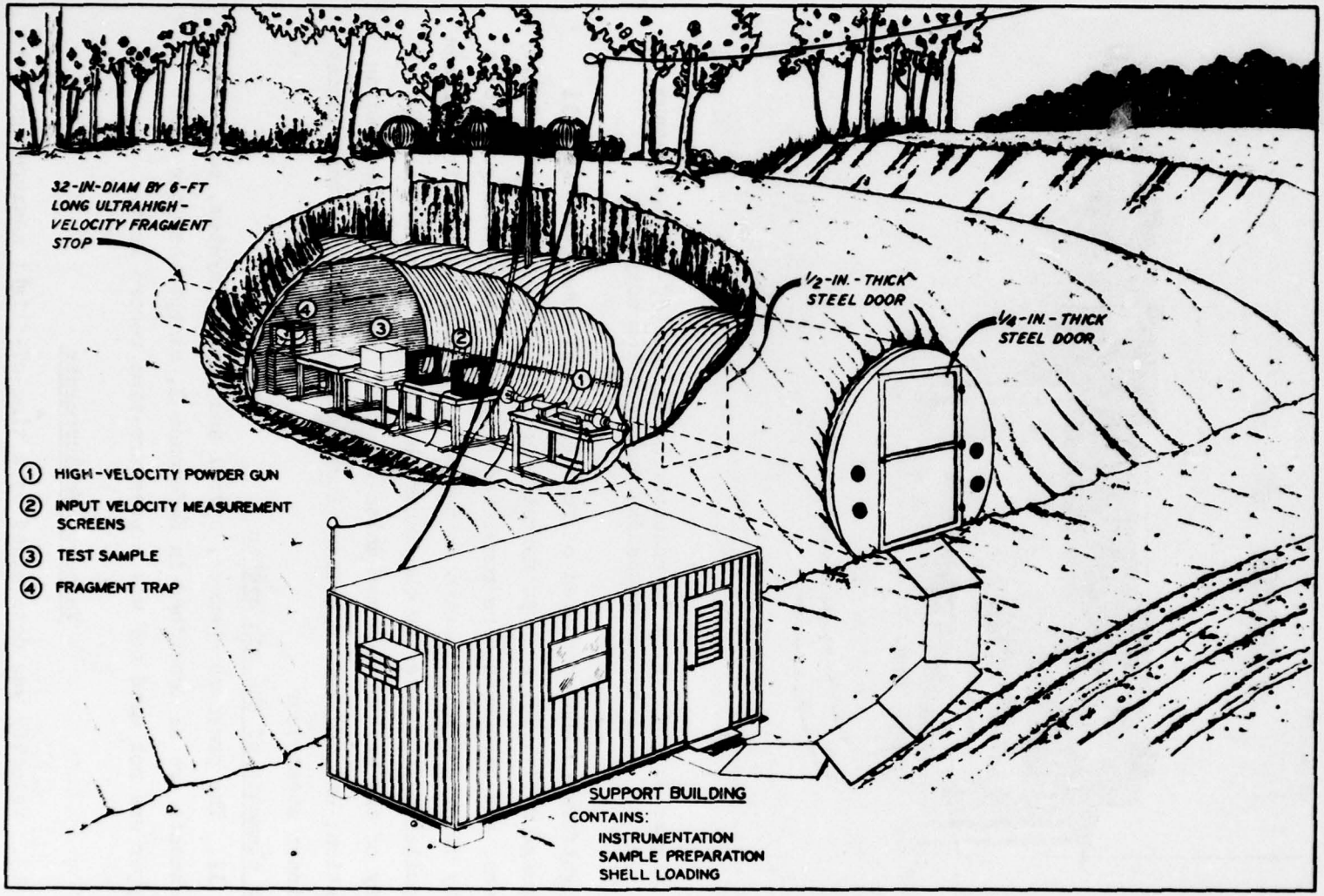

Figure 2. WES Fragment Simulation Facility

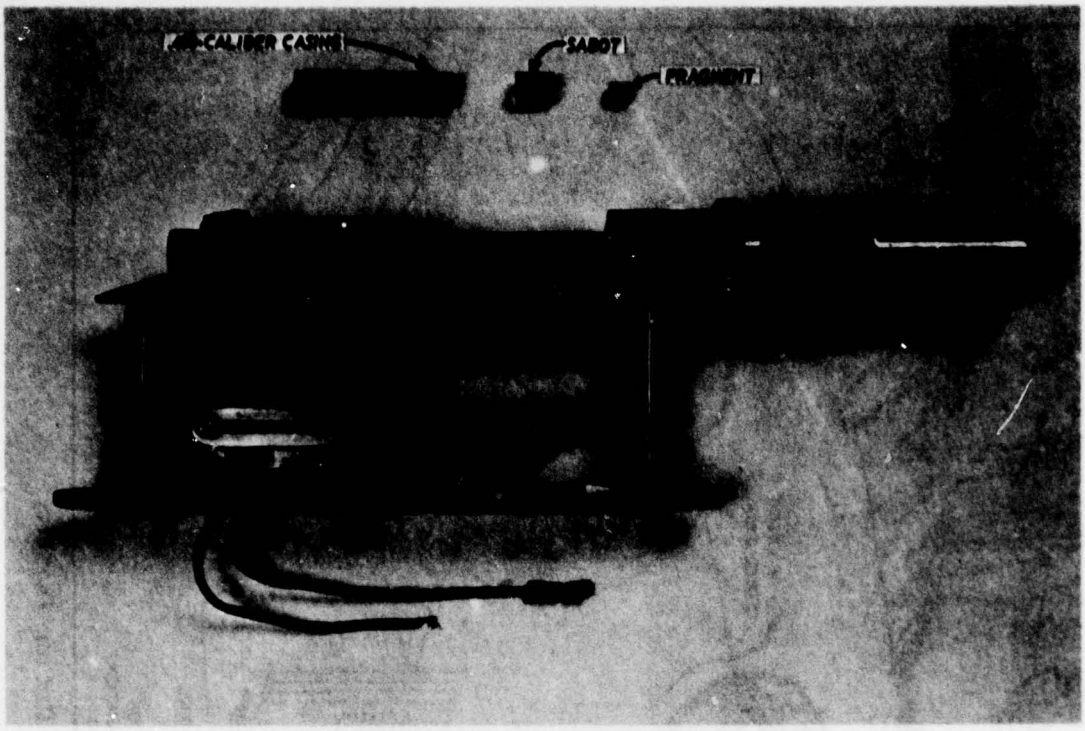

Figure 3. LV system (Winchester Model 70 .458-caliber magnum bolt-action mechanism and coupling adapter)

straightforward and consisted of four essential concepts: (a) all downrange activities such as target preparation, placement of velocity screens, and alignment were completed prior to loading the gun; (b) a safety interlock plug located in the outer chamber of the firing range was pulled before entering the inner chamber with a round; (c) the safety of the bolt-action mechanism was kept "on" during the loading operation; and (d) the interlock plus was replaced only after closing the inner steel door.

Other elements of the gun system

12. The pressure chamber, barrel and support system, and muzzle attachments are as described in Reference 3, except that the sabot stripper was not used nor was a pressure-time record kept.

Velocity Measurements

13. Velocity was determined by a time-of-flight measurement over

a known distance. Fragment velocities were measured using an Oehler Model 20 chronograph that measured the time period required for a fragment to travel between two photoelectric screens placed 4 ft apart. The time period, displayed in microseconds, was converted to velocity. This velocity was assumed to be the instantaneous velocity of the fragment at the center of the photoelectric screens (previous experiments with the photoelectric screens indicated that the error associated with this assumption is negligible). The setup for measuring the fragment velocity is shown in Figures 4 and 5. Data presented in References 2 and 3

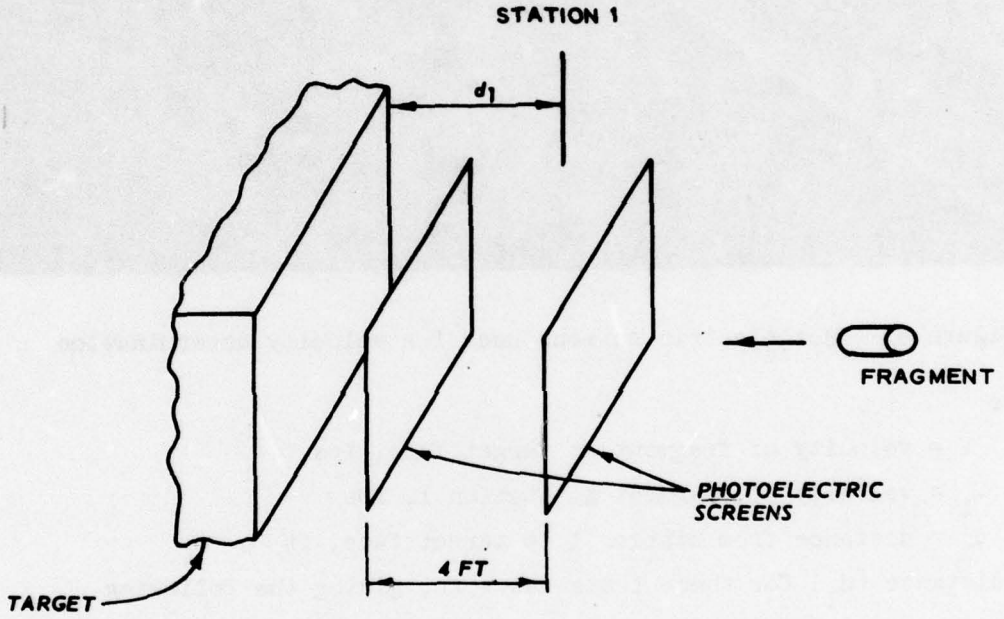

Figure 4. Setup for velocity determination

indicated that the actual velocity of the fragment (V*) at the front of the target could be determined from the velocity (V_1) measured at station 1 by using the relation

$$V = V_1 (1 - 0.005d_1) \qquad (1)$$

---

* For convenience, symbols and unusual abbreviations are listed and defined in the Notation (Appendix B).

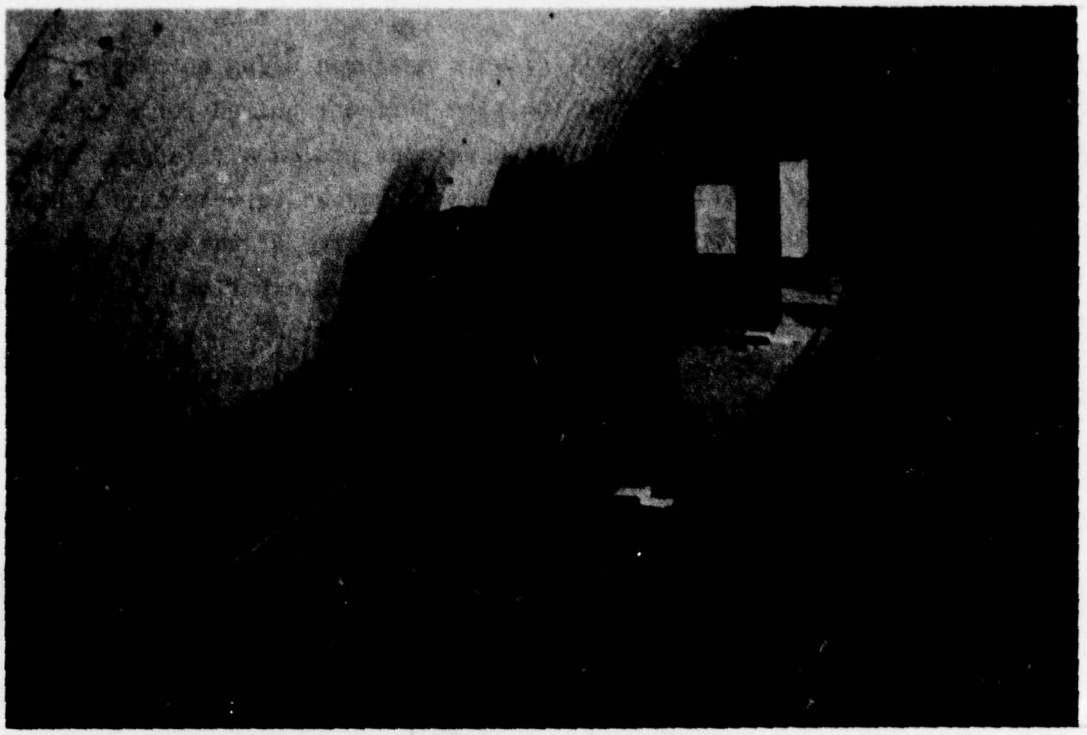

Figure 5. Photoelectric screens used for velocity determination

where

V = velocity of fragment at target face, fps

V_1 = velocity of fragment at station 1, fps

d_1 = distance from station 1 to target face, ft

The distance (d_1) for these tests was 4 ft, giving the following relation

$$V = 0.98V_1 \tag{2}$$

for determining the impact velocity of the fragment. Equations 1 and 2 assume a linear variation of V with distance traveled by the fragment.

14. The impulse energy imparted to the target was varied in the test by varying the impact velocity of the fragments, which were of constant mass. The impact velocity varied according to the powder charge weight in the cartridge. Figure 6 is a plot of the velocity (V_1) at station 1 (4 ft from the muzzle) versus powder charge weight for the system.

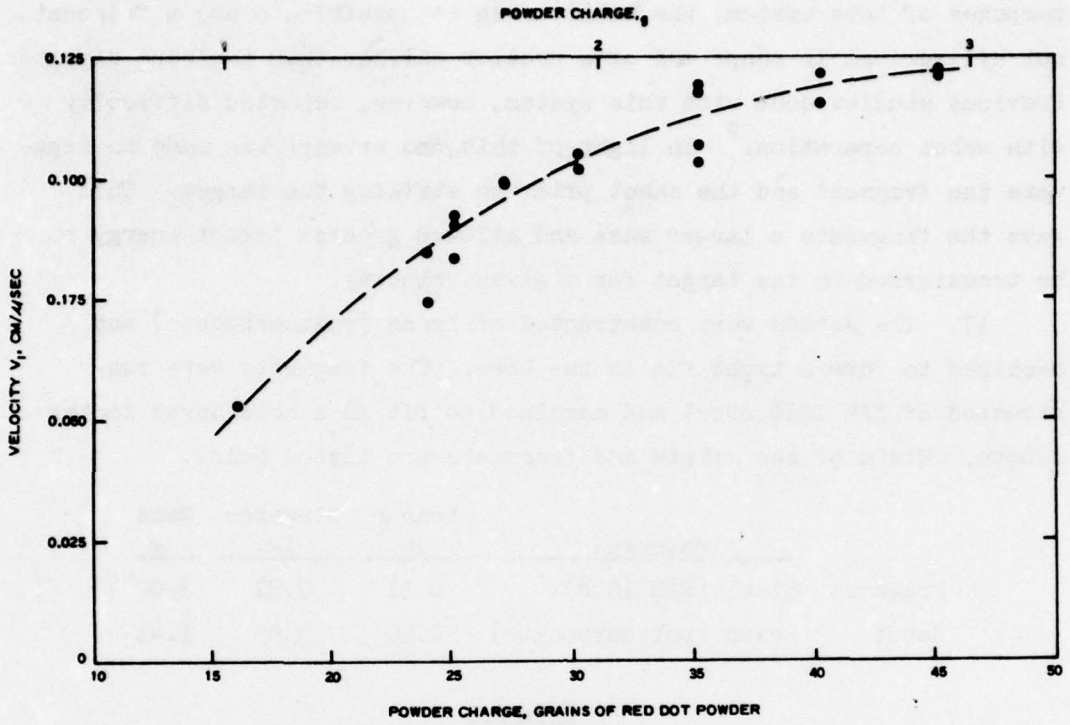

Figure 6. Velocity calibration for LV system (velocity at station 1)

Sabots and Fragments

15. As indicated in Reference 1, the size, mass, impact velocity, and areal distribution of fragments produced by artillery and mortar projectile detonation depends on such factors as explosive type, the ratio of projectile weight to charge weight, and the part of the projectile from which they originate. This information must be available to accurately predict the impulse imparted to a structure by the fragment. For the purposes of this study, right-circular cylindrical projectiles were used to simulate the fragments. Steel was selected for the fragments because its material properties approximated the properties of observed artillery and mortar fragments.[2]

16. A sabot is, by definition, a device which carries the fragment down the gun bore and then separates from the fragment, thus allowing a higher fragment velocity to be attained. In addition, for the

purposes of this system, the sabot makes it possible to use a fragment not cylindrical in shape and of a smaller caliber than the bore diameter. Previous studies done with this system, however, reported difficulty with sabot separation.[2] In light of this, no attempt was made to separate the fragment and the sabot prior to striking the target. This gave the fragments a larger mass and allowed greater impact energy to be transferred to the target for a given velocity.

17. The sabots were constructed of lexan (polycarbonate) and machined to form a tight fit in the bore. The fragments were constructed of SAE 1018 steel and machined to fit in a hole bored in the sabots. Sizes of the sabots and fragments are listed below.

	Material	Length in.	Diameter in.	Mass g
Fragment	Steel (SAE 1018)	0.31	0.31	3.00
Sabot	Lexan (polycarbonate)	0.50	0.45	1.41

Targets

18. Targets consisted of a concrete slab with an earth covering. Due to constraints of the gun system, it was necessary for the target to be situated vertically, with the fragment being fired horizontally at the target. The target and covering were attached to a reaction structure which provided a simply supported loading situation for the target, convering container, and reaction structure are shown in Figure 7.

Concrete roof slab

19. For the target, it was decided to model a precast concrete panel command and control shelter as described in Reference 4. The construction plans for this shelter are shown in Figure 8. The roof panel can be modeled using the Buckingham-Pi modeling laws as presented in Reference 5. In this study, it was decided to utilize a scale factor of one-eighth for all dimensions in the model. Thus the scaled roof slab had dimensions of 12 in by 13.5 in. by 0.75 in. and was mounted on the reaction structure with the 12-in. dimension vertical.

20. A sand-aggregate concrete mix with an average 9-day compressive strength of 3500 psi was used to simulate the 28-day 3000-psi

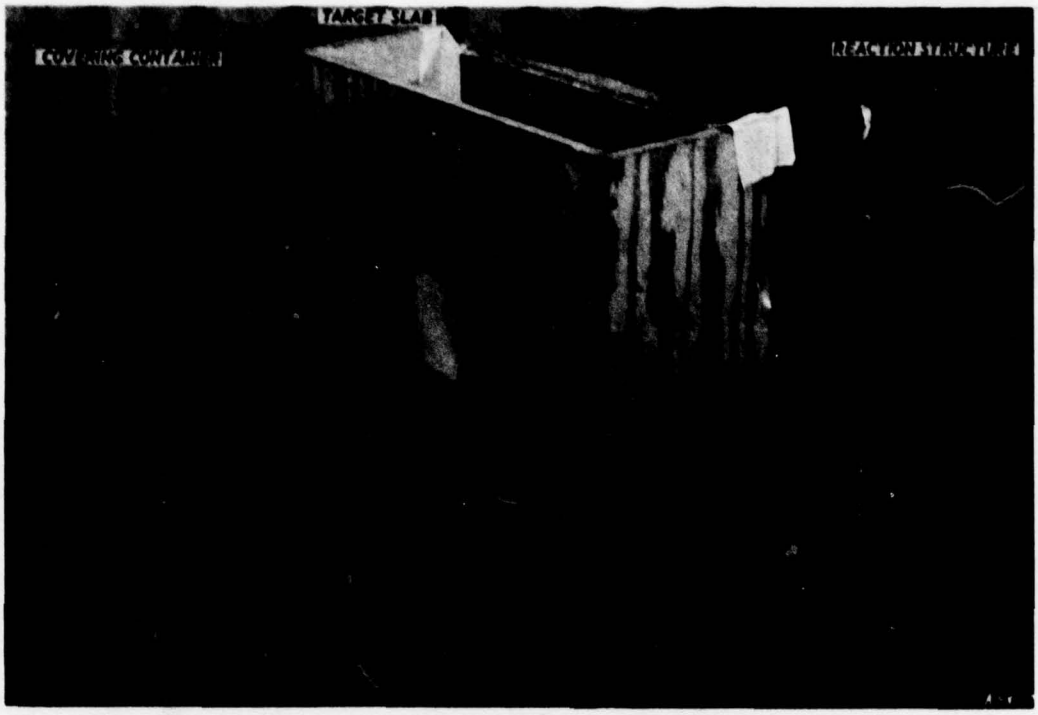

Figure 7. Target and reaction structure

concrete normally used for the shelter. The No. 4 reinforcing bars were simulated using 14-gage steel wire which had been annealed at a temperature of 1100°F for approximately 1 hour to reduce the yield strength to 40 ksi, which approximated the yield strength of Grade 40 reinforcing steel. To provide a bonding surface, the wire was allowed to rust slightly before the slabs were cast. The reinforcing steel and the casting form are shown in Figure 9. The lifting loops shown in Figures 8 and 9 were used to attach the slab to the reaction structure.

Covering

21. The covering was used primarily to prevent the fragment from impacting and penetrating the slab, as this would cause scabbing and/or spalling which would change the properties of the slab. In order to remain within the bounds of the modeling procedure and to maintain the same proportions of the prototype slab, a covering depth of approximately 4-1/2 in. was desired. The cover material was chosen to stop the fragment well within this region and also to provide a somewhat

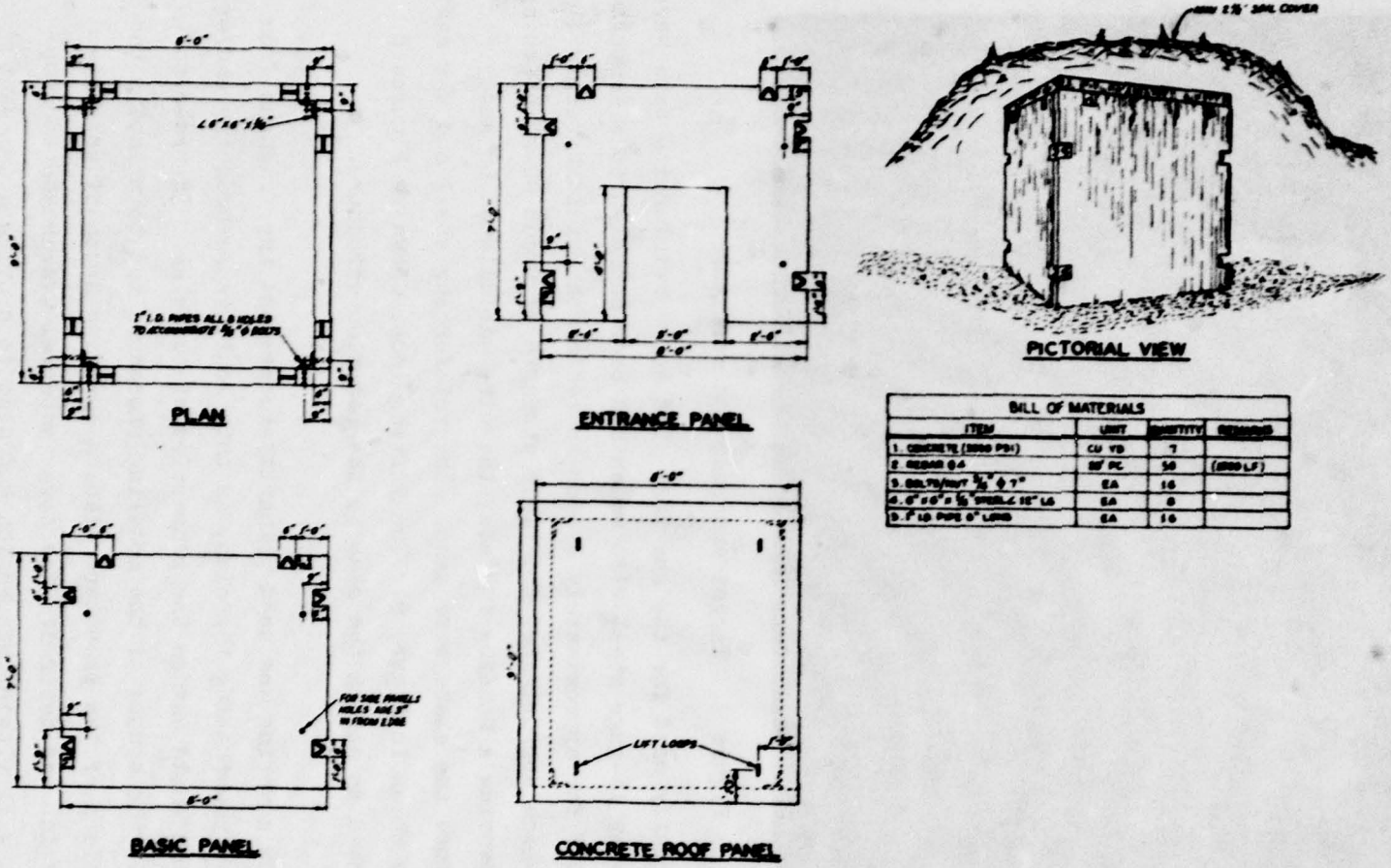

Figure 8. Construction plans for precast concrete panel command and control shelter

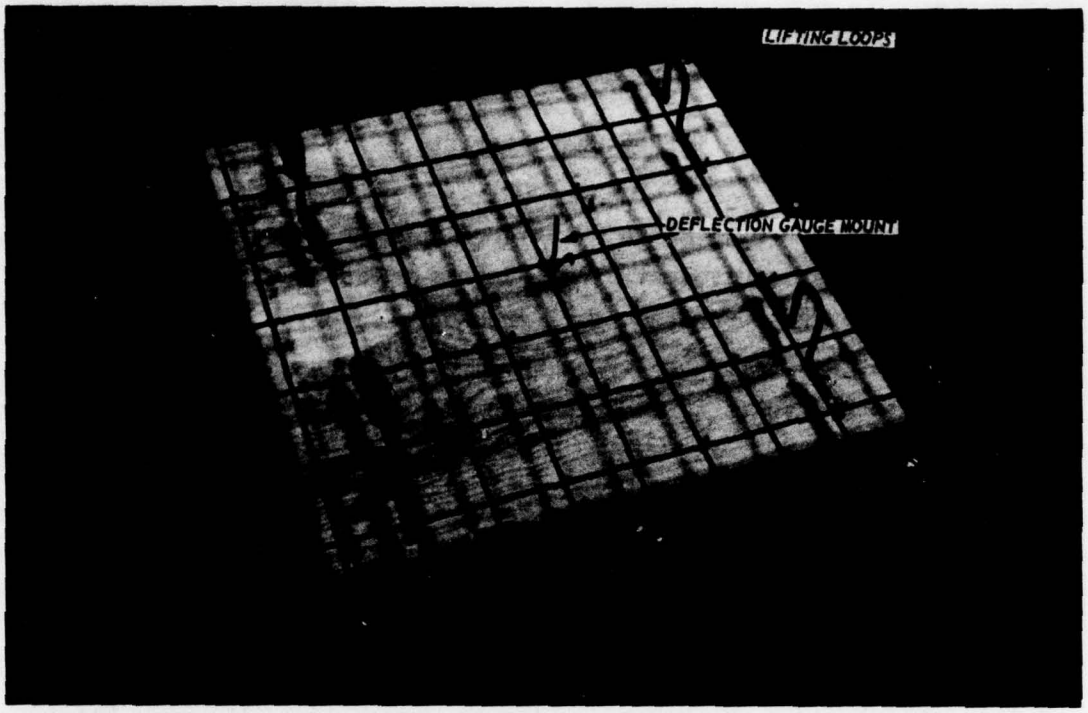

Figure 9. Reinforcing layout and form for target slab

consistent mixture. Based on the data in References 2 and 3, a dense sand was chosen as the cover material. In the target preparation, the sand was put in the container (Figure 7) in 3-in. layers, and each layer was compacted using a 5-lb impact hammer dropped 10 times from a height of 6 in. This method produced a covering with an approximate density of 100-105 pcf. One shot was fired into the target and then the fragment was recovered from the sand and the container refilled.

Test Results

22. The test results are given in Table 1 and include the impact velocity, maximum measured deflection, ductility ratio, and natural period of the response. The shot numbers identify the chronological order in which the fragments were fired. The maximum deflection and natural period are shown in Figure 1, which is a deflection-versus-time history of the center of the slab following impact.

PART III: ANALYTIC RESPONSE PREDICTION

Target Characteristics

23. A procedure is given in Reference 6 for representing a beam or one-way slab as an equivalent single-degree-of-freedom (SDOF) system for analysis and design purposes. This procedure involves using a series of transformation factors based on the load-support characteristics of the system to reduce it to a SDOF system.

Load Approximation

24. The fragment impact on the target is approximated by a concentrated load at the point of impact. In this study, the point of impact is the center of the slab. The slab is represented as a one-way slab, or beam, simply supported on its two long sides, the span being the short side. Table 2 presents the transformation factors and equations for developing the equivalent SDOF system.

Analytic Procedure

25. The procedure for analyzing the target system for an impulse load is outlined in Reference 7. It has been determined that the duration of load due to the fragment impact is larger than 10 times the natural period of the slab; therefore, an impulsive loading situation is assumed.* The impulsively loaded SDOF system is assumed to have the bilinear resistance function shown in Figure 10. The system has a stiffness

$$K = \frac{48EI}{L^3} \tag{3}$$

---

* The load duration is assumed to be the time needed to stop the fragment in the covering. In this study, this value had an upper bound of 0.001 sec, while the period was measured to be 0.011 sec.

as given in Table 2, where

K = stiffness

E = Young's modulus

I = second moment of beam cross-sectional area

L = span length of beam

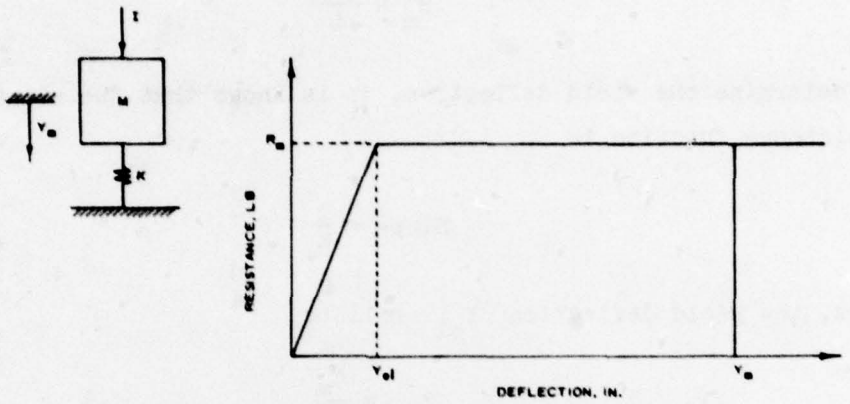

Figure 10. Impulsively loaded SDOF system and its bilinear resistance

The natural frequency is then calculated by:

$$\omega = \sqrt{\frac{K}{K_{LM} M}} \tag{4}$$

where

ω = natural frequency

K_{LM} = load mass factor (from Table 2)

M = mass of the system (slab + covering)

The ultimate moment capacity of the beam (M_p) is calculated by the equation

$$M_p = \rho_s \, bd^2 \, \sigma_y \left(1 - \frac{\rho_s \, \sigma_y}{1.7\sigma'_c}\right) \tag{5}$$

where

ρ_s = ratio of cross-sectional areas of steel to concrete

b = width of beam

d = depth of beam

σ_y = yield strength of steel reinforcing

σ'_c = concrete compressive strength

From Table 2 and Equation 5, the maximum resistance (R_m) is determined by the equation

$$R_m = \frac{4M_P}{L} \tag{6}$$

To determine the yield deflection, it is known that the slope of the resistance function is

$$\text{Slope} = \frac{1}{K}$$

thus, the yield deflection Y_{el} will be

$$Y_{el} = \frac{R_m}{K} \tag{7}$$

From Reference 7, the ductility ratio (μ), defined as the ratio of maximum deflection (Y_m) to elastic deflection (Y_{el}), is determined by the equation

$$\mu = \frac{1}{2}\left[\left(\frac{i\omega}{R_m}\right)^2 + 1\right] \tag{8}$$

where

i = fragment impulse

The fragment impulse (i) is given by the relation

$$i = m_f V$$

where

m_f = mass of the fragment

Knowing the ductility ratio from Equation 8, the maximum deflection due to the impulsive load is

$$Y_m = \mu Y_{el} \tag{9}$$

Response Prediction

26. The response of the slab to different impact loads was predicted by use of the analytic procedure described above. The response calculations are presented in Appendix A for review purposes.

Comparison of Analytic Procedure and Experimental Results

27. The experimental results and the results of the analytical work presented in Appendix A are shown in Figure 11. The experimental results appear to diverge from the analytic results as the impulse increases; however, the lack of data points prevents the prediction of any definite correlation or lack thereof. This divergence, however, may have been produced because the higher impulse shots were fired after some permanent deformation of the slab had taken place. This permanant deformation, when added to the response deflections, could have caused strain hardening, which in turn might have changed the properties of the slab. A crack was noticed to have developed following shot 8. The crack had propagated the full width of the slab and had penetrated nearly the full thickness of it (Figure 12). A static load-deflection test was conducted to obtain a resistance function for the slab following cracking. The yield deflection determined from this static test was 0.038 in. and was used to calculate the second values of the ductility ratio for shots 7, 8, and 9 noted in Figure 11 and in Table 1.

28. In determining the ductility ratio for the experimental results, the analytically derived yield deflection was used, since an experimental value could not be determined. Based on comparisons of the experimental and analytical yield loads and natural frequencies,

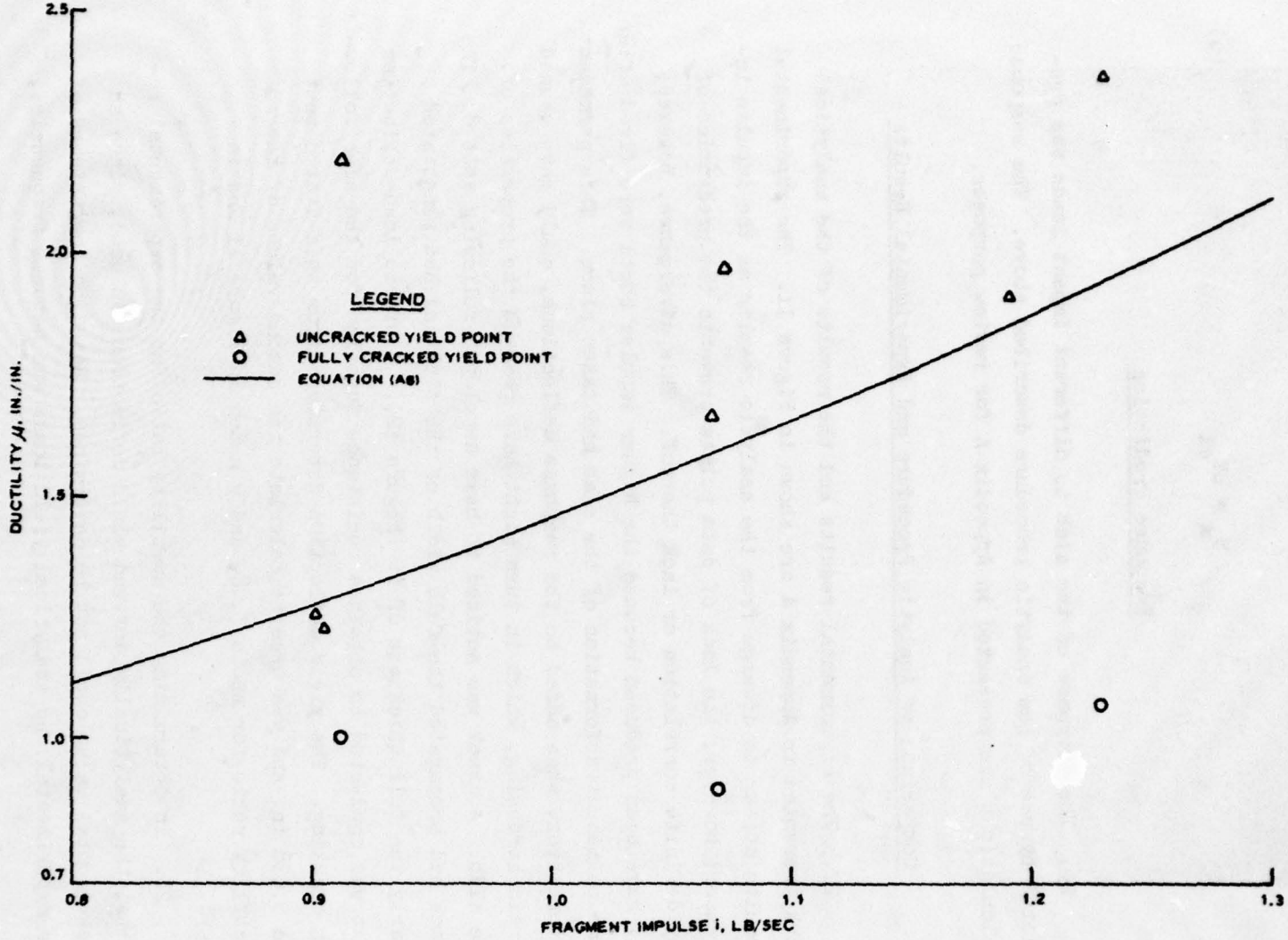

Figure 11. Comparison of experimental and analytical results

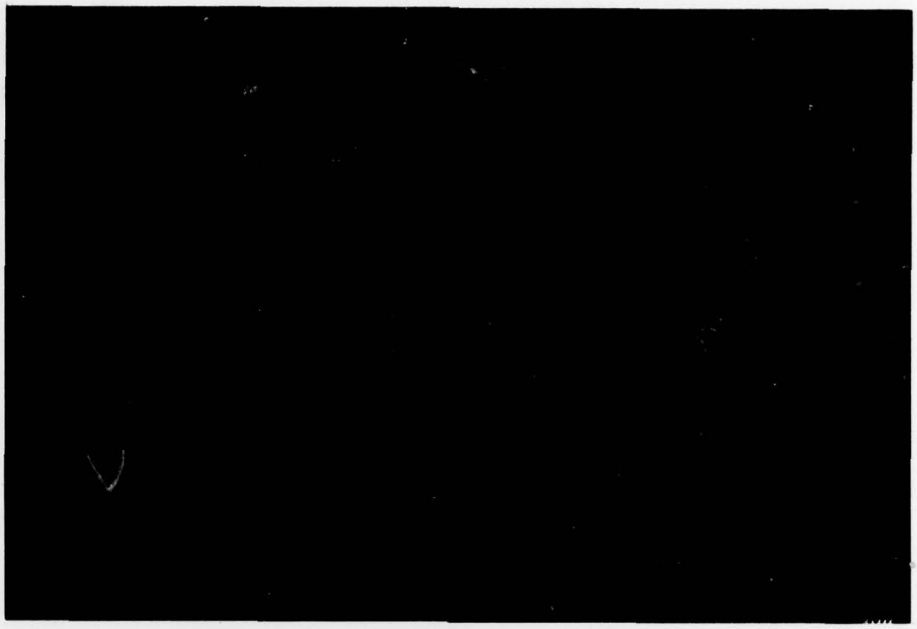

a. Front or impact side of slab

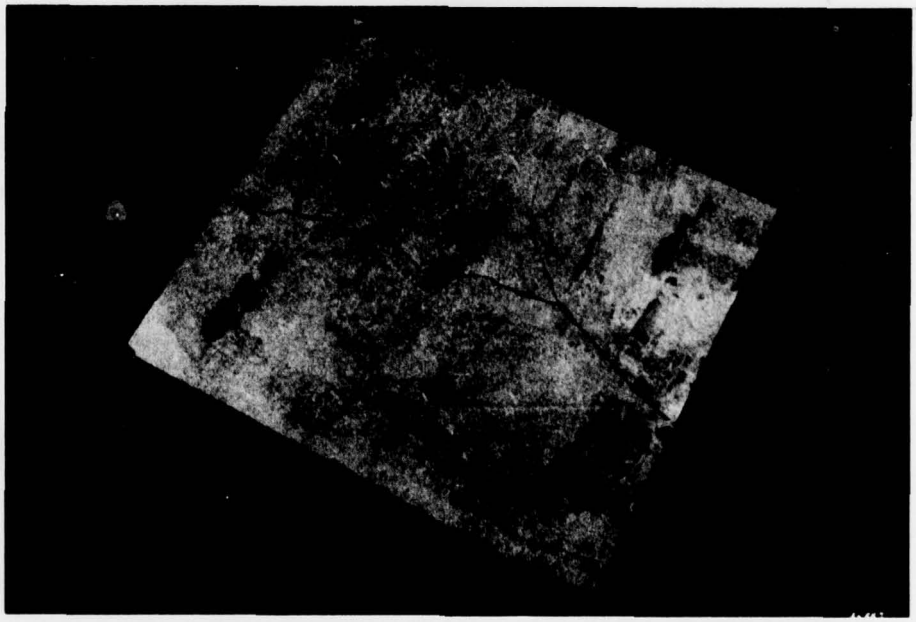

b. Rear of slab

Figure 12. Damage to slab after shot 8

the decision was made to use this value for the yield deflection because the natural frequency and yield load showed close predictions for the stiffness and load characteristics.

PART IV: CONCLUSIONS AND RECOMMENDATIONS

Conclusions

29. Based on the results of the experimental and theoretical work in the area of response to fragment impact, the conclusions are as follows:

a. Structural elements may be modeled by a SDOF system using the transformation factors outlined in Reference 6.

b. The equations introduced by Biggs[7] appear to be a good means for predicting maximum deflections from fragment impact.

30. The accuracy of the analytical work presented in this study is highly dependent on the loading condition assumed for the impact situation. There were insufficient data from this preliminary study, however, to make any significant correlation between the concentrated load assumption and the experimental results.

Recommendations

31. From considerations of soil dynamics, stress wave propagation, and impact mechanics, it becomes apparent that the loading condition is dependent on the soil covering depth, or the ratio of the soil covering depth to the fragment penetration depth. It is recommended that experimental work be done to determine the relationship between the soil cover depth and the loading condition.

32. As a guide for further experimental work in this area, it is recommended that a more accurate determination of the material properties of the concrete slab be made.

33. In analyzing the experimental procedure of this study, questions were raised concerning the effect of any permanent deformation on the results. Further work should be done to determine this effect before an analytical design procedure is developed.

REFERENCES

1. Kakel, W. W., "Fragment Defeating Capabilities of Plastic Armor," Technical Report N-71-10, Jun 1971, U. S. Army Engineer Waterways Experiment Station, CE, Vicksburg, Miss.

2. Rohani, B., "Fragment and Projectile Penetration Resistance of Soils; High-Velocity Fragment Penetration Into Laboratory Prepared Soil Targets," Miscellaneous Paper S-71-12, Report 2, Jun 1973, U. S. Army Engineer Waterways Experiment Station, CE, Vicksburg, Miss.

3. Butler, D., "Development of a High-Velocity Powder Gun and Analysis of Fragment Penetration Tests Into Sand," Miscellaneous Paper S-75-27, Oct 1975, U. S. Army Engineer Waterways Experiment Station, CE, Vicksburg, Miss.

4. Hoot, B. B. et al., "Evaluation of Field Fortifications," Technical Report N-74-5, Aug 1974, U. S. Army Engineer Waterways Experiment Station, CE, Vicksburg, Miss.

5. Canfield, J. A. and Clator, I. G., "Development of a Scaling Law and Techniques to Investigate Penetration in Concrete," Technical Report No. 2057, Aug 1966, U. S. Naval Weapons Laboratory, Dahlgren, Va.

6. Headquarters, Department of the Army, Office of the Chief of Engineers, "Design of Structures to Resist Atomic Weapons: Structural Elements Subjected to Dynamic Loads," Technical Manual No. 5-856-4, Dec 1965, Washingtion, D. C.

7. Biggs, J. M., Introduction to Structural Dynamics, McGraw-Hill, New York, 1964.

8. Norris, C. H. et al., Structural Design for Dynamic Loads, McGraw-Hill, New York, 1959.

Table 1

Experimental Results

Shot Number	Impact Velocity V fps	Maximum Deflection Y_m 10^{-2} in.	Ductility Ratio μ	Natural Period T msec
1*	--	--	--	--
2**	--	--	--	--
3	3528.4	2.867	1.66	10.1
4	3939.7	3.284	1.91	10.7
5	2994.6	2.109	1.22	11.6
6	2983.3	2.162	1.25	11.6
7	3547.5	3.396	1.97	10.8
7†	3547.5	3.396	0.89	10.8
8	4066.4	4.071	2.36	11.1
8†	4066.4	4.071	1.07	11.1
9	3017.7	3.758	2.19	10.2
9†	3017.7	3.758	1.00	10.2

* Misfire.
** No distinguishable deflection recorded.
† Ductility ratio calculated using fully cracked yield deflection.

Table 2

Equivalent Parameters for Beam and Slab Structures (from Reference 6)

Element	Equivalent Mass M_{eq}	Equivalent Stiffness K_{eq}	Equivalent Resistance R_{eq}	Load-Mass Factor K_{LM}
Concentrated load, simply supported beam	0.49M	$\frac{48EI}{L^3}$	$\frac{4M_P}{L}$	0.49

Note: E = Young's modulus; I = second moment of beam cross-sectional area; L = span length of beam; M = mass of beam and covering; M_P = ultimate moment capacity of beam.

APPENDIX A: ANALYTICAL PREDICTION OF DUCTILITY RATIO

1. Following the procedure presented in Part III, a prediction of the ductility ratio, as a function of the fragment impulse, can be calculated. Table A1 shows the values used in this calculation for the slab used in this study.

2. The equations and calculations are:

a. Mass determination.

$$M = \frac{\gamma_s bdL + \gamma_c t_c bL}{g}$$

$$= \frac{1 \text{ sec}^2}{386 \text{ in.}} \left(\frac{144 \text{ lb}}{\text{ft}^3} \times \frac{13.5 \text{ ft}}{12} \times \frac{0.75 \text{ ft}}{12} \times \frac{12 \text{ ft}}{12} \right.$$

$$\left. + \frac{100 \text{ lb}}{\text{ft}^3} \times \frac{4.75 \text{ ft}}{12} \times \frac{13.5 \text{ ft}}{12} \times \frac{12 \text{ ft}}{12} \right)$$

$$= \frac{0.14160 \text{ lb-sec}^2}{\text{in.}} \qquad \text{(A1)}$$

b. Moment. The second moment of the beam's cross-sectional area is determined using an average of the cracked and uncracked sections of the concrete slab. This value is used based on recommendations in References 7 and 8* and is calculated by the equation

$$I = \frac{bd^3}{2} (5.5 \rho_s + 0.083)$$

$$= \frac{13.5 \text{ in.} \times (0.75 \text{ in.})^3}{2} (5.5 \times 0.004468 + 0.083)$$

$$= 0.3063 \text{ in.}^4 \qquad \text{(A2)}$$

---

* Numbers refer to similarly numbered items in the References at the end of the main text.

c. Stiffness.

$$K = \frac{48EI}{L^3}$$

$$= 48 \times \frac{1}{(12\ \text{in.})^3} \times 3.0 \times 10^6\ \text{lb/in.}^2 \times 0.3063\ \text{in.}^4$$

$$= 25{,}525\ \text{lb/in.} \qquad \text{(A3)}$$

d. Natural frequency.

$$\omega = \sqrt{\frac{K}{K_{LM}M}}$$

$$= \sqrt{25{,}525\ \text{lb/in.} \times \frac{1}{0.49} \times \frac{1\ \text{in.}}{0.14160\ \text{lb-sec}^2}}$$

$$= 606.5\ \frac{1}{\text{sec}} \qquad \text{(A4)}$$

e. Ultimate moment capacity.

$$M_p = \rho_s b d^2 \sigma_y \left(1 - \frac{\rho_s \sigma_y}{1.7\sigma'_c}\right)$$

$$= (0.004468) \times 13.5\ \text{in.} \times (0.75\ \text{in.})^2$$

$$\times 40{,}000\ \text{lb/in.}^2 \times \left(1 - \frac{0.004468 \times 40{,}000\ \text{lb/in.}^2}{1.7 \times 3500\ \text{lb/in.}^2}\right)$$

$$= 1316.39\ \text{in.-lb} \qquad \text{(A5)}$$

f. Maximum resistance.

$$R_m = \frac{4M_p}{L}$$

$$= 4 \times 1316.39\ \text{in.-lb} \times \frac{1}{12\ \text{in.}} = 438.80\ \text{lb} \qquad \text{(A6)}$$

g. Yield deflection.

$$Y_{el} = \frac{R_m}{K}$$

$$= 438.80 \text{ lb} \times \frac{1 \text{ in.}}{25{,}525 \text{ lb}} = 0.01719 \text{ in.} \qquad \text{(A7)}$$

h. Ductility ratio.

$$\mu = \frac{1}{2}\left(\frac{i\omega}{R_m}\right)^2 + 1$$

$$= \frac{1}{2}\left[\left(\frac{606.5 \frac{1}{\text{sec}} \times i \text{ lb-sec}}{438.80 \text{ lb}}\right)^2 + 1\right]$$

$$= 0.9552\, i^2 + 0.5 \qquad \text{(A8)}$$

3. A graph of Equation A8 with the experimentally determined ductility ratios appears in Figure 11.

Table A1

Constants and Measured Values Used in Calculating the Ductility Ratio

Symbol	Value
Weight density of slab (γ_s)	= 144 lb/ft^3
Weight density of cover (γ_c)	= 100 lb/ft^3
Slab width (b)	= 13.5 in.
Slab thickness (d)	= 0.75 in.
Slab length (L)	= 12.0 in.
Cover thickness (t_c)	= 4.75 in.
Steel to concrete area ratio (ρ_s)	= 0.004468
Young's modulus (E)	= 3.0×10^6 lb/in.^{2}
Yield strength of steel (σ_y)	= 40,000 lb/in.^{2}
Compressive strength of concrete (σ_c')	= 3500 lb/in.^{2}

APPENDIX B: NOTATION

b	Slab width, in. or ft
d	Slab thickness, in. or ft
d_1	Distance from station 1 to target face, ft
E	Young's modulus of elasticity, psi
i	Fragment impulse, lb-sec
I	Second moment of slab cross-sectional area, $in.^4$
K	Stiffness, lb/in.
K_{LM}	Load mass factor
L	Span length, in. or ft
M	Mass of slab and soil cover, $lb\text{-}sec^2/in.$
m_f	Mass of fragment, $lb\text{-}sec^2/ft$
M_P	Ultimate moment capacity of slab, in.-lb
R_m	Maximum resistance, lb
T	Natural period, msec
t_c	Soil cover thickness on target, in.
V_1	Velocity of fragment at station 1, fps
V	Velocity of fragment at impact, fps
Y_{el}	Elastic limit deflection of center of slab, in.
Y_m	Maximum dynamic deflection at center of slab, in.
γ_c	Density of soil covering, lb/ft^3
γ_s	Density of slab, lb/ft^3
μ	Ductility ratio, Y_m/Y_{el}
ρ_s	Steel to concrete area ratio
σ_y	Yield strength of steel reinforcing, psi
σ'_c	Compressive strength of concrete, psi
ω	Natural frequency, $1/sec^2$

In accordance with letter from DAEN-RDC, DAEN-ASI dated 22 July 1977, Subject: Facsimile Catalog Cards for Laboratory Technical Publications, a facsimile catalog card in Library of Congress MARC format is reproduced below.

Lutman, Thomas R
Response of a model roof slab to fragment impact loading / by Thomas R. Lutman. Vicksburg, Miss. : U. S. Waterways Experiment Station ; Springfield, Va. : available from National Technical Information Service, 1979.
26, [6] p. : ill. ; 27 cm. (Miscellaneous paper - U. S. Army Engineer Waterways Experiment Station ; SL-79-14.
Prepared for Office, Chief of Engineers, U. S. Army, Washington, D. C., under Project 4A762719AT40, Task BO, Work Unit 002.
References: p. 26.

1. Concrete slabs. 2. Fortifications. 3. Impact tests. 4. Impulsive loads. 5. Roofs. 6. Slabs. 7. Structural members. 8. Structural models. 9. Weapon fragmentation. I. United States. Army. Corps of Engineers. II. Series: United States. Waterways Experiment Station, Vicksburg, Miss. Miscellaneous paper ; SL-79-14.
TA7.W34m no.SL-79-14